

See discussions, stats, and author profiles for this publication at: <https://www.researchgate.net/publication/221671712>

Polymer Detachment Kinetics from Adsorbing Surface: Theory, Simulation and Similarity to Infiltration into Porous Medium

ARTICLE in *MACROMOLECULES* · MARCH 2012

Impact Factor: 5.8 · DOI: 10.1021/ma202671n · Source: arXiv

CITATIONS

12

READS

16

4 AUTHORS, INCLUDING:



Andrey Milchev

Bulgarian Academy of Sciences

237 PUBLICATIONS 4,464 CITATIONS

SEE PROFILE



Vakhtang G. Rostiashvili

Max Planck Institute for Polymer Research

78 PUBLICATIONS 725 CITATIONS

SEE PROFILE



Thomas Vilgis

Max Planck Institute for Polymer Research

389 PUBLICATIONS 4,261 CITATIONS

SEE PROFILE

Polymer Detachment Kinetics from Adsorbing Surface: Theory, Simulation and Similarity to Infiltration into Porous Medium

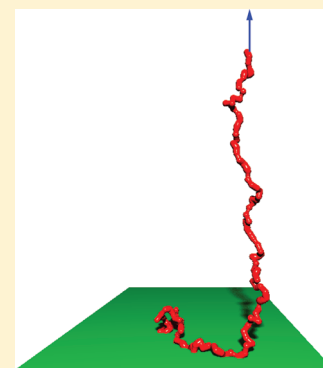
Jaroslav Paturej,^{†,‡,*} Andrey Milchev,^{†,§} Vakhtang G. Rostishvili,[†] and Thomas A. Vilgis[†]

[†]Max Planck Institute for Polymer Research, 10 Ackermannweg, 55128 Mainz, Germany

[‡]Institute of Physics, University of Szczecin, Wielkopolska 15, 70451 Szczecin, Poland

[§]Institute for Physical Chemistry, Bulgarian Academy of Science, 1113 Sofia, Bulgaria

ABSTRACT: The force-assisted desorption kinetics of a macromolecule from adhesive surface is studied theoretically, using the notion of tensile (Pincus) blobs, as well as by means of Monte Carlo (MC) and molecular dynamics (MD) simulations. We show that the change of detached monomers with time is governed by a differential equation which is equivalent to the nonlinear porous medium equation (PME), employed widely in transport modeling of hydrogeological systems. Depending on the pulling force and the strength of adsorption, three kinetic regimes can be distinguished: (i) “trumpet” (weak adsorption and small pulling force), (ii) “stem–trumpet” (weak adsorption and moderate force), and (iii) “stem” (strong adsorption and large force). Interestingly, in all regimes the number of desorbed beads $M(t)$, and the height of the first monomer (which experiences a pulling force) $R(t)$ above the surface follow an universal square-root-of-time law. Consequently, the total time of detachment $\langle\tau_d\rangle$, scales with polymer length N as $\langle\tau_d\rangle \propto N^2$. Our main theoretical conclusions are tested and found in agreement with data from extensive MC- and MD-simulations.



1. INTRODUCTION

During the past decade the progress in single-molecule manipulation techniques such as atomic force spectroscopy (AFM) and optical or magnetic tweezers¹ has attracted the interest of researchers to a new field of fascinating phenomena like DNA unzipping,^{2–4} or forced-induced detachment of individual polymers from adsorbing surfaces.⁵ One can experimentally test elastic and adhesive properties as well as bond scission in polymer fibers, or in fundamental biological objects like proteins, nucleic acids, or molecular motors with spatial resolution in the nm range and force resolution in the pN range. In this way substantial progress has been achieved in the understanding and use of fibers, adhesives or biopolymers. Besides technological relevance, the field of single-chain manipulation poses also numerous questions of interest to fundamental physics. Thus, it has been shown, for example, that the force-induced unzipping of the double-stranded DNA is a 1st order phase transition^{2,3,6,7} that has the same nature as the force-induced desorption transition of a polymer from an adhesive substrate^{8–11} and that both phenomena can be described by the same kind of *re-entrant* phase diagram.

While the theoretical understanding of these phase transformations in terms of equilibrium statistical thermodynamics has meanwhile significantly improved,¹¹ their kinetics has been so far less well explored. Originally, a theoretical treatment of the problem was suggested by Sebastian⁶ while the first computer simulations of the related phenomenon of DNA force-induced unzipping were reported by Marenduzzo et al.⁷ Yet a number of basic questions pertaining to the dependence of the total mean detachment time $\langle\tau_d\rangle$ on polymer length N , pulling force f , or adhesion strength, ε_s , remain open or need

validation. So far we are not aware of computer simulational studies which would shed light on these problems. Therefore, in order to fill the gap regarding force-induced desorption kinetics, we consider in this work a generic problem: the force-induced detachment dynamics of a single chain, placed on adhesive structureless plane.

The theoretical method which we used is different and more general than in ref 6, where a phantom (Gaussian) chain was treated in terms of the corresponding Rouse equation. Instead, our consideration (i) takes into account all excluded-volume interactions among monomers and (ii) is based on the tensile-blob picture, proposed many years ago by Brochard-Wyart¹² as theoretical framework for the description of a steady-state driven macromolecule in solutions. This approach was generalized recently by Sakaue^{13,14} for the analysis of nonequilibrium transient regimes in polymer translocations through a narrow pore.

Very recently, Sebastian et al.¹⁵ demonstrated (within the tensile blob picture) that the average position $x(n,t)$ of a monomer n at time t is governed by the so-called p -Laplacian nonlinear diffusion equation.¹⁶ In contrast, in the present paper we discuss force-induced desorption kinetics on the basis of a nonlinear diffusion equation which governs the time-dependent density distribution $\rho(x,t)$ of monomers. We show that this equation is similar to the *porous medium equation* (PME)¹⁷ which has gained widespread acceptance in the theory of groundwater transport through geological strata.¹⁸ The most

Received: December 9, 2011

Revised: April 20, 2012

Published: May 1, 2012

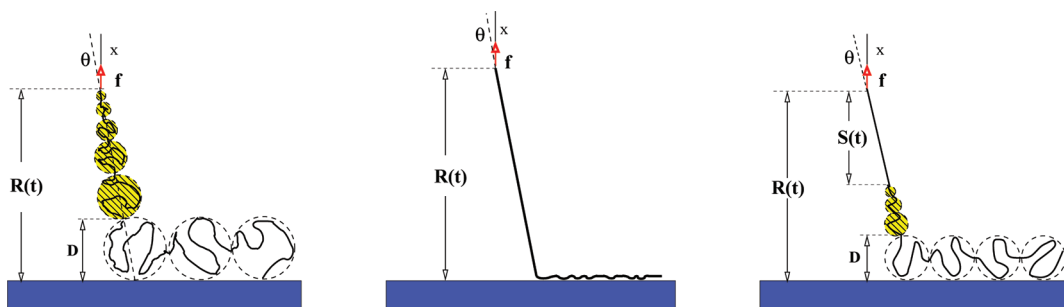


Figure 1. The picture of the single adsorbed chain detachment. The chain is initially equilibrated, giving rise to a string of adsorption blobs with a blob size D . The external driving force f , exerted on the first monomer, is switched on at the initial time moment. By time t the position of the first monomer is denoted as $R(t)$. The shaded part of the chain displays a tensile blobs sequence which has a form of a “trumpet”, tilted opposite to the lateral velocity direction by angle θ . (a) The “trumpet” regime, corresponding to weak adsorption and weak pulling force, i.e., $1/N^\nu \ll \tilde{\varphi} < \tilde{f} < 1$. (b) The “stem” regime, corresponding to strong adsorption and strong pulling force, $1 \ll \tilde{\varphi} < \tilde{f}$. (c) The “stem–trumpet” regime, representing the intermediate pulling force interval $\tilde{\varphi} < 1 < \tilde{f}$.

natural way of solving the PME is based on *self-similarity* which implies that the governing equation is invariant under the proper space and time transformation.^{17,18} Thus, self-similarity reduces the problem to a nonlinear ordinary differential equation which can be solved much more easily.

Eventually, in order to check our predictions we performed extensive MD- and MC-simulations which, for the case of strong adsorption, large pulling forces and overdamped regime, show an excellent agreement with our theoretical predictions. Moreover, the comparison of MC and MD data reveals that the presence of inertial effects, typical in underdamped dynamics, significantly affects the observed detachment kinetics.

The paper is organized as follows: after this short introduction, in section 2, we present briefly the theoretical treatment of the problem and emphasize the different regimes pertinent to polymer detachment kinetics. A short description of the simulational MC- and MD models is given in section 3 while in section 4, we discuss the main results provided by our computer experiments. We end this work by a brief summary of our findings in section 5.

2. TENSILE-BLOB PICTURE FOR THE FORCE-INDUCED DETACHMENT

2.1. Trumpet Regime. *2.1.1. Beads Density Temporal Variation Is Described by a Nonlinear Porous Medium Equation.* After equilibration on an attractive solid substrate, the adsorbed polymer chain can be pictured as a two-dimensional string of *adsorption blobs* of size $D \propto a(\varepsilon_s - \varepsilon_c)^{-\nu/\phi}$,¹⁹ where a is the Kuhn segment length, and ν and ϕ are respectively the Flory exponent and the crossover (or, adsorption) exponent. The dimensionless adsorption energy $\varepsilon_s = \varepsilon_s/k_B T$ (here and in what follows k_B denotes the Boltzmann constant, and T is temperature), whereas ε_c is the critical adsorption point (CAP). The external driving force f acts on the free chain end (in the x -direction) while the second chain end is tethered to the substrate. If the pulling force strength falls in the range $1/N^\nu \ll af/k_B T \leq 1$, the chain tail forms a kind of “trumpet” shape, as shown schematically in Figure 1a. Moreover, as far as the adsorption blob, adjacent to “trumpet”, changes its lateral position (i.e., its coordinates within the substrate) during desorption, the “trumpet” has not only vertical velocity (in the x -direction) but also a lateral one. The latter leads to a tilt of the “trumpet” axis in direction opposite to the lateral velocity due to Stokes friction. The tilting angle is denoted by θ in Figure 1 and, as will be seen from our

simulation results in section 4, almost does not change in the course of detachment. This substantially simplifies the theoretical consideration.

Let us denote by $f(x, t)$ the tensile force which acts in direction of the “trumpet” axis at an arbitrary cross-section of a tensile (Pincus) blob, placed at distance x from the substrate at time t . The x -component of this tensile force reads $f_x(x, t) = f(x, t) \cos \theta$. The blob size is then given by

$$\xi(x, t) = \frac{k_B T}{f(x, t)} = \frac{C k_B T}{f_x(x, t)} \quad (1)$$

where $C = \cos \theta$. It can be seen from Figure 1a that the size of the tensile blob at x corresponds to the lateral size of the polymer at height x . The balance of forces in x -direction at this point yields

$$f_x(x, t) = \gamma \int_D^x v_x(x', t) \left[\frac{\xi(x', t)}{a} \right]^{z-2} \frac{dx'}{\xi(x', t)} + \varphi \quad (2)$$

where $v_x(x, t)$ is the x -component of the local velocity and φ is the *restoring force* which is exerted on the moving domain by the last adsorption blob. The value of φ depends on the proximity to the critical point ε_c as well as on the chain model itself (see below). In the integral in eq 2, $dx'/\xi(x', t)$ counts the number of blobs in the interval $x', x' + dx'$ whereas $\gamma v_x(x', t) [\xi(x', t)/a]^{z-2}$ is the local Stokes friction force (γ being the friction coefficient).²⁰ The dynamic exponent equals either $z = 2 + 1/\nu$, or $z = 3$, for Rouse and Zimm dynamics, respectively. Thus, taking into account eq 1, the equation for the blob size reads

$$\xi(x, t) = \frac{C k_B T}{\gamma \int_D^x v_x(x', t) [\xi(x', t)/a]^{z-2} dx' / \xi(x', t) + \varphi} \quad (3)$$

With this equation one may represent the local velocity $v(x, t)$ in terms of the blob size $\xi(x, t)$ as

$$v_x(x, t) = -\frac{C k_B T}{a \gamma} \left[\frac{a}{\xi(x, t)} \right]^{z-1} \frac{\partial \xi(x, t)}{\partial x} \quad (4)$$

The local (linear) monomer density $\rho(x, t)$ and the local blob size $\xi(x, t)$ are related by $\rho(x, t) = [\xi(x, t)/a]^{(1-\nu)/\nu}$ so that eq 4 can be written in the form

$$v_x(x, t) = -\frac{Ck_B T \nu}{\gamma(1-\nu)} \frac{1}{[\tilde{\rho}(x, t)]^{\nu(z-2)/(1-\nu)+1}} \frac{\partial \tilde{\rho}(x, t)}{\partial x} \quad (5)$$

where we have introduced the notation for the dimensionless monomer density $\tilde{\rho}(x, t) = a\rho(x, t)$.

The local flux of polymer beads has a standard form $J_x(x, t) = v_x(x, t) \rho(x, t)$, that is

$$J_x(x, t) = -\frac{\nu Ck_B T}{a\gamma(1-\nu)[\tilde{\rho}(x, t)]^{\nu(z-2)/(1-\nu)+1}} \frac{\partial \tilde{\rho}(x, t)}{\partial x} \quad (6)$$

With $J_x(x, t)$ from eq 6, one may determine $\tilde{\rho}(x, t)$ from the continuity equation $\partial \rho(x, t) / \partial t = -\partial J_x(x, t) / \partial x$:

$$\frac{\partial \tilde{\rho}}{\partial \tilde{t}} = \frac{\partial}{\partial \tilde{x}} \left(\tilde{\rho}^{m-1} \frac{\partial \tilde{\rho}}{\partial \tilde{x}} \right) \quad (7)$$

where we have introduced the dimensionless (tilded) independent variables $\tilde{x} = x/a$ and $\tilde{t} = t/\tau_0$ (thereby the characteristic time is $\tau_0 = a^2\gamma(1-\nu)/\nu Ck_B T$). Equation 7 has the form of the nonlinear *porous medium equation* (PME)¹⁷ where the characteristic exponent $m = -[\nu(z-1)-1]/(1-\nu)$ has in our case a negative value. An equation similar to PME has been discussed recently by Sakaue et al.²¹ in the context of polymer expansion and unfolding from a compact state. In this case the consideration has been based on the dynamics of *concentration blobs*²⁰ rather than tensile blobs like here. This kind of nonlinear partial differential (parabolic) equations is commonly used in the context of groundwater infiltration or seepage through porous strata¹⁸ where the exponent $m > 1$.

The geometric factor $C = \cos \theta$ is unessential in the subsequent consideration and we will drop it. In addition to eq 7, one has to fix the initial and boundary conditions (BC). Initially, there are no polymer segments at $x > D$, so that

$$\tilde{\rho}(x, t = 0) = 0 \quad (8)$$

At $x = D$ the tensile blob is equal in size to the adsorption blob, i.e., $\xi(x = D, t) = k_B T / \varphi$. As a result, in terms of the dimensionless density, one has

$$\tilde{\rho}(\tilde{x} = \tilde{D}, t) = \frac{1}{\tilde{\varphi}^{(1-\nu)/\nu}} \quad (9)$$

where $\tilde{D} = D/a$ and $\tilde{\varphi} = a\varphi/k_B T$.

The BC on the moving end of the “trumpet” follows from the condition $\xi(x = R(t), t) = k_B T / f$ which corresponds to the smallest blob size, i.e.,

$$\tilde{\rho}(\tilde{x} = \tilde{R}(t), t) = \frac{1}{\tilde{f}^{(1-\nu)/\nu}} \quad (10)$$

Here again the dimensionless quantities, $\tilde{R}(t) = R(t)/a$ and $\tilde{f} = af/k_B T$, are introduced.

Our consideration is based on the assumption that the lateral component of the tensile force is very weak (because the trumpet is almost vertical), so that any force propagation along the adsorbed part of chain can be neglected. This is different from the case considered by Serr and Netz²² where the pulling of a strongly adsorbed chain by means of an AFM has been investigated. In contrast to the present case where an uniform field pulls on the first bead, the AFM cantilever can move vertically and horizontally with respect to substrate so that the tilt angle θ changes with time. Moreover, in this case the sliding of the polymer on the substrate becomes important with the

polymer–surface friction force being much larger than the Stokes friction force for the detached part which is essential in our case. Therefore, the AFM can not be actually used for testing the scheme shown in Figure 1.

2.1.2. Self-Similar Solution. In the same manner as for the PME, the solution of eq 7 is derived by symmetry of self-similarity (SS). This symmetry implies invariance of the solution with respect to the *stretching transformation*: $\tilde{t} \rightarrow \eta \tilde{t}$, $\tilde{x} \rightarrow \eta^\delta \tilde{x}$, $\tilde{\rho} \rightarrow \eta^\omega \tilde{\rho}$. The requirement that eq 7 stays invariant under the stretching transformation connects the exponents ω , m , and δ by the following relation¹⁷

$$\omega(1-m) + 2\delta = 1 \quad (11)$$

On the other hand, this requirement also fixes the self-similar form of the solution as

$$\tilde{\rho}(\tilde{x}, \tilde{t}) = t^\omega W(u), \quad u = (\tilde{x} - \tilde{D})/\tilde{t}^\delta \quad (12)$$

In eq 12, $W(u)$ is a scaling function and we took into account that at $\tilde{t} = 0$ $\tilde{x} = \tilde{D}$. On the other hand, the boundary condition given by eq 9 is compatible with the SS-form eq 12 only if $\omega = 0$. Then, as a consequence of eq 11, $\delta = 1/2$. Substituting eq 12 into 7 yields a nonlinear ordinary differential equation for the scaling function $W(u)$, i.e.

$$\frac{d}{du} \left(W^{m-1} \frac{dW}{du} \right) + \frac{u}{2} \frac{dW}{du} = 0 \quad (13)$$

The BC given by eq 9 reads

$$W(u = 0) = \frac{1}{\tilde{\varphi}^{(1-\nu)/\nu}} \quad (14)$$

Assume now that the moving chain end follows the scaling relation $\tilde{R}(\tilde{t}) = \tilde{D} + \tilde{v}_d \tilde{t}^\chi$ where χ is an exponent and the factor \tilde{v}_d will be fixed below. This scaling ansatz is compatible with the BC given by eq 10 only if $\chi = 1/2$. This imposes the boundary condition

$$W(u = \tilde{v}_d) = \frac{1}{\tilde{f}^{(1-\nu)/\nu}} \quad (15)$$

Finally, the initial condition eq 8 becomes

$$W(u = \infty) = 0 \quad (16)$$

The nonlinear eq 13 may be solved numerically. However, in case the pulling force f exceeds the restoring force only by a small amount, one can show (see below) that $\tilde{v}_d \ll 1$, i.e., the interval of argument u variation, where $W(u)$ is nonzero, is very narrow. As a result, $0 \leq u\tilde{v}_d \ll 1$ and one can linearize eq 13 (by making use eq 14) to get

$$\tilde{\varphi}^{z-2} \frac{d^2}{du^2} W(u) + \frac{u}{2} \frac{dW}{du} = 0 \quad (17)$$

where for small arguments $W(u)^{m-1} \approx \tilde{\varphi}^{(z-2)}$. The solution of eq 17, subject to both conditions eq 14 and eq 16, is given by

$$W(u) = \frac{1}{\tilde{\varphi}^{(1-\nu)/\nu}} \left[1 - \operatorname{erf} \left(\frac{u}{2\tilde{\varphi}^{(z-2)/2}} \right) \right] \quad (18)$$

where $\operatorname{erf}(x) = (2/\sqrt{\pi}) \int_0^x \exp(-t^2) dt$ is the error function.

The chain end velocity amplitude, \tilde{v}_d , can be determined now from the condition eq 15. If the pulling force \tilde{f} is only slightly larger than the restoring force $\tilde{\varphi}$, one can expand $W(u) \approx [1 - u/(\pi^{1/2} \tilde{\varphi}^{(z-2)/2})]/\tilde{\varphi}^{(1-\nu)/\nu}$. Thus, one obtains

$$\tilde{v}_d \simeq \sqrt{\pi} \tilde{\varphi}^{(z-2)/2} \left[1 - \left(\frac{\tilde{\varphi}}{\tilde{f}} \right)^{(1-\nu)/\nu} \right] \quad (19)$$

The equation of motion for the moving end then reads

$$\tilde{R}(\tilde{t}) = \tilde{D} + \sqrt{\pi} \tilde{\varphi}^{(z-2)/2} \left[1 - \left(\frac{\tilde{\varphi}}{\tilde{f}} \right)^{(1-\nu)/\nu} \right] \sqrt{\tilde{t}} \quad (20)$$

The variation of the number of desorbed monomers with time, $M(t)$, is given by the integral

$$\begin{aligned} M(t) &= \int_D^{R(t)} \rho(x, t) dx \\ &= \sqrt{\tilde{t}} \int_0^{\tilde{v}_d} W(u) du \\ &\simeq \sqrt{\pi} \tilde{\varphi}^{(z-2)/2\nu} \left[1 - \left(\frac{\tilde{\varphi}}{\tilde{f}} \right)^{(1-\nu)/\nu} \right] \sqrt{\tilde{t}} \end{aligned} \quad (21)$$

Eventually, the total time for polymer detachment, $\langle \tau_d \rangle$, reads

$$\langle \tau_d \rangle = \frac{\tau_0 N^2}{\pi \tilde{\varphi}^{(z-2)/2\nu} [1 - (\tilde{\varphi}/\tilde{f})^{(1-\nu)/\nu}]^2} \quad (22)$$

Combining eqs 21 and 22, one obtains the following dynamical scaling law

$$M(t) = N \sqrt{\frac{\tilde{t}}{\langle \tau_d \rangle}} \quad (23)$$

Eventually, we would like to stress that in the foregoing consideration one neglects the thermal fluctuations so that the necessary condition for desorption requires that $\tilde{f} > \tilde{\varphi}$. On the other hand, the “trumpet” formation is only possible when $1/N^\nu \ll \tilde{f} < 1$. Therefore, the “trumpet” regime holds, provided that

$$1/N^\nu \ll \tilde{\varphi} < \tilde{f} < 1 \quad (24)$$

which means that then one deals with weak adsorption and weak pulling force.

2.2. Dependence of the Restoring Force φ on the Adsorption Energy ε_s . One can write the restoring force in scaling form, $\varphi = k_B T / \mathcal{F}(\varepsilon_s)$, with $\varepsilon_s = \varepsilon_s / k_B T$ and $\mathcal{F}(x)$ —a scaling function. Force φ stays constant in the course of the desorption process as long as at least one adsorption blob is still located on the attractive surface. The strength of φ can be determined from the plateau in the deformation curve: force vs chain end position.²³

In an earlier work,²⁴ we demonstrated that the fugacity per adsorbed monomer $z^*(\varepsilon_s)$, which determines its chemical potential $\mu_{\text{ads}} = \ln z^*$, can be found from the basic equation

$$\Phi(\alpha, \mu_3 z^*) \Phi(\lambda, \mu_2 w z^*) = 1 \quad (25)$$

In eq 25, $\alpha = \phi - 1$ (ϕ is the so-called crossover exponent which, according to the different simulation methods, ranges between $\phi \simeq 0.48$ and $\phi \simeq 0.59$; see the corresponding discussion in ref 24) $\lambda = 1 - \gamma_{d=2} \simeq -0.343$ (where $\gamma_{d=2}$ is a universal exponent which governs the two-dimensional polymer statistics), $w = \exp(\varepsilon_s)$, μ_2 , and μ_3 are so-called *connective constants* in two- and three-dimensional spaces respectively, and the polylog function Φ is defined by the series $\Phi(\alpha, y) = \sum_{n=1}^{\infty} y^n / n^\alpha$.

n^α . The values of μ_2 , μ_3 and $\gamma_{d=2}$ could be found in the textbook.²⁵

In local equilibrium μ_{ads} should be equal to the chemical potential of detached monomer $\mu_{\text{det}} = (1/k_B T)(\partial F_{\text{str}}/\partial N)$, where F_{str} is the free energy of the *driven* polymer chain so that $\mu_{\text{ads}} = \mu_{\text{det}}$. The expression for F_{str} depends on the polymer model. The moving blob domain, shown in Figure 1, exerts on the last adsorbed monomer a force which is equal in magnitude and opposite in sign to the restoring force φ . Therefore, the free energy of a stretched polymer within the *bead-spring* (BS) model is given by²⁴

$$F_{\text{str}} = -N \left(\frac{a\varphi}{k_B T} \right)^{1/\nu} - N \ln \mu_3 \quad (26)$$

On the other hand, within the freely jointed bond vector (FJBV) model, the partition function, corresponding to F_{str} , reads²⁶

$$Z_N = (4\pi)^N \left(\frac{k_B T}{a\varphi} \right)^N \left[\sinh \left(\frac{a\varphi}{k_B T} \right) \right]^N \quad (27)$$

In eq 27 the free chain partition function $Z_N = (4\pi)^N$ for $\varphi \rightarrow 0$. A correspondence with the BS-model may be established by the substitution $4\pi \rightarrow \mu_3$ in eq 27 so that the FJBV-free energy becomes

$$F_{\text{str}} = -k_B T N \ln \left[\mu_3 \left(\frac{k_B T}{a\varphi} \right) \sinh \left(\frac{a\varphi}{k_B T} \right) \right] \quad (28)$$

Taking into account eqs 26 and 28, one obtains eventually

$$\frac{a\varphi}{T} = \begin{cases} [-\ln(\mu_3 z^*(\varepsilon_s))]^\nu, & \text{BS model} \\ \mathcal{R}^{-1}(-\ln(\mu_3 z^*(\varepsilon_s))), & \text{FJBV model} \end{cases} \quad (29)$$

where $\mathcal{R}^{-1}(x)$ is the inversed of the function $\mathcal{R}(x) = \ln[\mu_3 \sinh(x)/x]$ and $\mu_3 z^*(\varepsilon_s) \leq 1$.

Below we consider separately the restoring force, eq 29, in the limits of strong and weak adsorption.

2.2.1. Strong Adsorption. In the case of the strong adsorption ($\varepsilon_s \gg 1$), the solution of eq 25 reads $z^*(\varepsilon_s) \simeq \mu_2^{-1} e^{-\varepsilon_s}$,²⁴ and for the BS-model one gets $a\varphi/k_B T \simeq [\varepsilon_s + \ln(\mu_2/\mu_3)]^\nu$.

For the FJBV model at $\varepsilon_s \gg 1$ one has $\mathcal{R}(x) \simeq \ln(\mu_3 e^x/x) \simeq x + \ln \mu_3$. From eq 29 it then follows $a\varphi/k_B T + \ln \mu_3 = \varepsilon_s + \ln \mu_2$, or $a\varphi/k_B T \simeq \varepsilon_s + \ln(\mu_2/\mu_3)$. The final result for the restoring force in the strong adsorption limit takes on the form

$$\tilde{\varphi} = \begin{cases} [\varepsilon_s + \ln(\mu_2/\mu_3)]^\nu, & \text{BS model} \\ \varepsilon_s + \ln(\mu_2/\mu_3), & \text{FJBV model} \end{cases} \quad (30)$$

It is well-known that under strong forces (and correspondingly strong adsorption) the FJBV-model is better suited for description of the simulation experiment results (see, e.g., section 5 in ref 23). That is why, in eq 30, the second line appears to be the more appropriate result.

2.2.2. Weak Adsorption. Close to the critical adsorption point, the solution of eq 25 takes on the form $z^*(\varepsilon_s) \simeq \mu_3^{-1} [1 - C_1(\varepsilon_s - \varepsilon_c)^{1/\phi}]$,²⁴ where C_1 is a constant. Then, eq 29 gives $a\varphi/k_B T \simeq C_1(\varepsilon_s - \varepsilon_c)^{\nu/\phi}$ for the BS-model.

In the case of weak adsorption $a\varphi/k_B T$ is small and $\mathcal{R}(x) \simeq \ln[\mu_3(1 + x^2/6)] \simeq \ln \mu_3 + x^2/6$. Equation 29 then yields $a\varphi/$

$k_B T \simeq B_1(\varepsilon_s - \varepsilon_c)^{1/2\phi}$, where B_1 is a constant. The unified result in the weak adsorption limit is

$$\tilde{\varphi} = \begin{cases} C_1(\varepsilon_s - \varepsilon_c)^{\nu/\phi}, & \text{BS model} \\ B_1(\varepsilon_s - \varepsilon_c)^{1/2\phi}, & \text{FJBV model} \end{cases} \quad (31)$$

In fact, eq 31 may also be derived differently. Namely, as already mentioned, the size of an adsorption blob is given by $D = aC_1(\varepsilon_s - \varepsilon_c)^{-\nu/\phi}$ whereas the size of a tensile blob $\xi(x = D) = k_B T/\varphi$. The condition for detachment may be set as $\xi(x = D) = D$ which leads again to eq 31 (whereby the dimensionless notation $\tilde{\varphi} = a\varphi/k_B T$ has been used). On the other hand, the relationship between D and φ , written as $D\varphi/k_B T \simeq 1$, leads to the adsorption blob size for the FJBV-model: $D \sim (\varepsilon_s - \varepsilon_c)^{-1/2\phi}$ (where the second line in eq 31 has been used).

2.3. Stem and Stem–Trumpet Regimes. For strong, $1 < a\varphi/k_B T < a\tilde{f}/k_B T$, and moderate, $a\varphi/k_B T < 1 < a\tilde{f}/k_B T$, detachment force f one has to consider the “stem” (see Figure 1b) and “stem–trumpet” (see Figure 1c) regimes, respectively.

2.3.1. Stem Regime. In this case the moving domain is build up from a “stem” of the length $M(t)$ (total number of desorbed monomers). The “stem” velocity is $dM(t)/dt$ (with an accuracy of the geometrical factor $C = \cos\theta$ which is not important for scaling predictions), so that the balance of driving and drag forces yields

$$\gamma M(t) \frac{dM(t)}{dt} = f - \varphi \quad (32)$$

The solution of eq 32 in the dimensionless units reads

$$M(t) = \sqrt{2(\tilde{f} - \tilde{\varphi})\tilde{t}} \quad (33)$$

Evidently, this takes on the same form as eq 23, $M(t) = N(\tilde{t}/\langle \tilde{\tau}_d \rangle)^{1/2}$, whereby the mean detachment (dimensionless) time $\langle \tilde{\tau}_d \rangle = N^2/[2(\tilde{f} - \tilde{\varphi})]$.

2.3.2. Stem–Trumpet Regime. The “stem–trumpet” shape of the driven polymer is shown in Figure 1c. In this case the local density in the “trumpet” part $\tilde{\rho}(\tilde{x}, \tilde{t})$ is governed by the same eq 7 but with a boundary condition in the junction point (i.e., in the point where the “stem” goes over into the “trumpet” part). There, the blob size is $\xi(x = R(t) - S(t), t) = a$. Thus, one gets

$$\tilde{\rho}(\tilde{x} = \tilde{R}(t) - \tilde{S}(t), \tilde{t}) = 1 \quad (34)$$

The boundary condition at $\tilde{x} = \tilde{D}$ has the same form, eq 9, as before. The solution again has the scaling form $\tilde{\rho}(\tilde{x}, \tilde{t}) = W(u)$. The moving end now follows the law $\tilde{R}(t) = \tilde{D} + \tilde{S}(t) + \tilde{u}_d \sqrt{\tilde{t}}$, where the prefactor \tilde{u}_d can be fixed by using the condition $W(u = \tilde{u}_d) = 1$. Consequently,

$$\tilde{u}_d = \sqrt{\pi} \tilde{\varphi}^{(z-2)/2} [1 - \tilde{\varphi}^{(1-\nu)/\nu}] \quad (35)$$

In order to calculate the length of the “stem” portion, $\tilde{S}(t)$, one can use the results of the previous subsection. The only difference lies in the fact that now the “stem–trumpet” junction point moves itself with velocity $\tilde{u}_d/(2\sqrt{\tilde{t}})$ and the driving force is $\tilde{f} - 1$. Therefore, the balance of driving and drag forces leads to the following equation for $\tilde{S}(t)$

$$\left(\frac{\tilde{u}_d}{2\sqrt{\tilde{t}}} + \frac{d}{d\tilde{t}} \tilde{S}(t) \right) \tilde{S}(t) = \tilde{f} - 1 \quad (36)$$

The solution of eq 36 reads

$$\tilde{S}(t) = \left[\sqrt{\frac{\tilde{u}_d^2}{4} + 2(\tilde{f} - 1)} - \frac{\tilde{u}_d}{2} \right] \sqrt{\tilde{t}} \quad (37)$$

The resulting equation for the average height of the end monomer becomes

$$\tilde{R}(t) = \tilde{D} + \left[\sqrt{\frac{\tilde{u}_d^2}{4} + 2(\tilde{f} - 1)} + \frac{\tilde{u}_d}{2} \right] \sqrt{\tilde{t}} \quad (38)$$

The number of desorbed monomer can be easily calculated as an integral over the number of monomers in the “trumpet” part and in the “stem” portion, i.e.

$$\begin{aligned} M(\tilde{t}) &= \sqrt{\tilde{t}} \int_0^{\tilde{u}_d} W(u) du + \tilde{S}(\tilde{t}) \\ &= \left[\sqrt{\frac{\tilde{u}_d^2}{4} + 2(\tilde{f} - 1)} - \frac{\tilde{u}_d}{2} \left(1 - \frac{2}{\tilde{\varphi}^{(1-\nu)/\nu}} \right) \right] \sqrt{\tilde{t}} \end{aligned} \quad (39)$$

where \tilde{u}_d is given by eq 35. Evidently, all characteristic scales as well as the number of desorbed monomers vary in time as \sqrt{t} . This shows that the average desorption time $\langle \tau \rangle$ is proportional to N^2 as before.

2.4. Dynamic Regimes. The foregoing theoretical analysis was based essentially on the notion of tensile (Pincus) blobs as well as on the “quasi-static” approximation, i.e., on the equating of driving and drag forces locally (in space and time). Depending on the pulling \tilde{f} and restoring $\tilde{\varphi}$ force strengths, one distinguishes a “trumpet” ($1/N^\nu \ll \tilde{\varphi} < \tilde{f} < 1$), “stem–trumpet” ($\tilde{\varphi} < 1 < \tilde{f}$), and a “stem” ($1 < \tilde{\varphi} < \tilde{f}$) regimes (see Figure 2). Notably, in all regimes the average number of

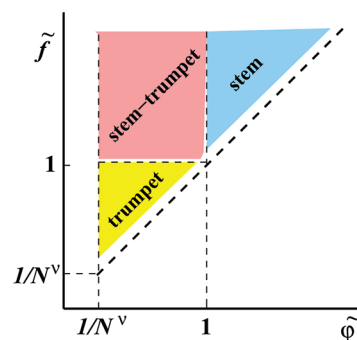


Figure 2. Different dynamic regimes of forced polymer chain desorption in terms of pulling \tilde{f} and restoring $\tilde{\varphi}$ forces. The relation between $\tilde{\varphi}$ and the adsorption energy ε_s is given by eq 30 and eq 31 for the strong and weak adsorption, respectively. The white strip along the diagonal indicates that in all cases the condition $\tilde{f} > \tilde{\varphi}$ is important.

desorbed monomers $M(t)$ and the height of the first monomer $R(t)$ evolve as a \sqrt{t} -time universal law. Moreover, the evolution equation which governs the polymer beads density $\rho(x, t)$ in the tensile blobs is analogous to the nonlinear porous medium equation which is commonly used for investigations of gas and fluid infiltration in the geological porous strata.^{17,18} Following this line we have demonstrated that the scaling analysis of such equation, based on symmetry of self-similarity, immediately brings about a \sqrt{t} -time universal law.

The value of $\tilde{\varphi}$ depends on the adsorption energy ε_s and is described by different expressions, depending on the particular

polymer chain model: bead–spring (BC), or freely jointed bond vectors (FJBV) models. For large adsorption energy ($\varepsilon_s \gg 1$), the restoring force is also large, leading to the “stem” regime. Close to the critical adsorption point (for vanishing adhesion), the restoring force could attain a very small value, leading to a ‘trumpet’ or “stem–trumpet” regime. In this case the role of fluctuations, which was neglected in our theoretical investigation, becomes important and could result in correction to the basic \sqrt{t} -time law.

In the next section we will give results of our MC- and MD-simulation study that were carried out in some of the foregoing forced-desorption (mainly “stem”) regimes.

3. COMPUTATIONAL MODELS

3.1. Monte Carlo. We have used a coarse grained off-lattice bead spring model to describe the polymer chains. Our system consists of a single chain tethered at one end to a flat structureless surface while the external pulling force is applied to other chain end. In the MC simulation the surface attraction of the monomers is described by a square well potential $U_w(x) = -\varepsilon_s$ for $x < \delta = 0.125$ and $U_w(x) = 0$ otherwise. Here the strength $\varepsilon_s/k_B T$ is varied from 0.6 to 3.6. The effective bonded interaction is described by the FENE (finitely extensible nonlinear elastic) potential.

$$U_{\text{FENE}} = -K(1 - l_0)^2 \ln \left[1 - \left(\frac{l - l_0}{l_{\text{max}} - l_0} \right)^2 \right] \quad (40)$$

with $K = 20$, $l_{\text{max}} = 1$, $l_0 = 0.7$, $l_{\text{min}} = 0.4$

The nonbonded interactions between the monomers are described by the Morse potential.

$$\frac{U_M(r)}{\varepsilon_M} = \exp(-2\alpha(r - r_{\text{min}})) - 2 \exp(-\alpha(r - r_{\text{min}})) \quad (41)$$

with $\alpha = 24$, $r_{\text{min}} = 0.8$, $\varepsilon_M/k_B T = 1$. This model is currently well established and has been used due to its reliability and efficiency in a number of studies²⁷ of polymer behavior on surfaces.

We employ periodic boundary conditions in the $y - z$ directions and impenetrable walls in the z direction. The lengths of the studied polymer chains are typically 64, 128, and 256. The size of the simulation box was chosen appropriately to the chain length, so for example, for a chain length of 128, the box size was $256 \times 256 \times 256$. All simulations were carried out for constant force. A force f was applied to the last monomer in the x -direction, i.e., perpendicular to the adsorbing surface

The standard Metropolis algorithm was employed to govern the moves with self-avoidance automatically incorporated in the potentials. In each Monte Carlo update, a monomer was chosen at random and a random displacement was attempted with Δx , Δy , Δz chosen uniformly from the interval $-0.5 \leq \Delta x, \Delta y, \Delta z \leq 0.5$. The transition probability for the attempted move was calculated from the change ΔU of the potential energies before and after the move as $W = \exp(-\Delta U/k_B T)$. As for standard Metropolis algorithm, the attempted move was accepted, if W exceeds a random number uniformly distributed in the interval $[0, 1]$. As a rule, the polymer chains have been originally equilibrated in the MC method for a period of about 10^6 MCS (depending on degree of adsorption ε_s and chain length N this period is varied) whereupon one performs 200 measurement runs, each of length 8×10^6 MCS. Various properties of the chain are then sampled during the course of the run. The starting configuration is replaced by a new sequence in the beginning of the next run. Two typical snapshots of chain configurations, immediately before the detachment starts, and some time later, are presented in Figure 3.

3.2. Molecular Dynamics. In our MD-simulations we use a coarse-grained model of a polymer chain of N beads connected by finitely extendable elastic bonds. The bonded interactions in the chain is described by the frequently used Kremer-Grest potential, $V^{\text{KG}}(r) = V^{\text{FENE}}(r) + V^{\text{WCA}}(r)$, with FENE potential, eq 40, and a nonbonded

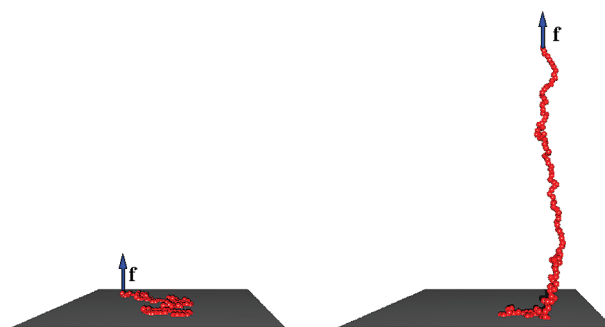


Figure 3. Snapshots from a MC simulation of chain with $N = 128$, adsorbed on a solid plane with energy of adsorption $\varepsilon_s/k_B T = 3.0$, at time $t = 0$ (a) before and (b) after a pulling force $f = 3.0$ is applied perpendicular to substrate.

repulsion term taken as Weeks–Chandler–Anderson (WCA) (i.e., the shifted and truncated repulsive branch of the Lennard-Jones potential) given by

$$V^{\text{WCA}}(r) = 4\varepsilon[(\sigma/r)^{12} - (\sigma/r)^6 + 1/4]\theta(2^{1/6}\sigma - r) \quad (42)$$

with $\theta(x) = 0$ or 1 for $x < 0$ or $x \geq 0$, and $\varepsilon = 1$, $\sigma = 1$. The potential $V^{\text{KG}}(r)$ has got a minimum at bond length $r_{\text{bond}} \approx 0.96$.

The substrate in the present investigation is considered simply as a structureless adsorbing plane, with a Lennard-Jones potential acting with strength ε_s in the perpendicular x -direction, $V^{\text{LJ}}(x) = 4\varepsilon_s[(\sigma/x)^{12} - (\sigma/x)^6]$.

The dynamics of the chain is obtained by solving a Langevin equation of motion for the position $\mathbf{r}_n = [x_n, y_n, z_n]$ of each bead in the chain,

$$m\ddot{\mathbf{r}}_n = \mathbf{F}_n^j + \mathbf{F}_n^{\text{WCA}} - \gamma\dot{\mathbf{r}}_n + \mathbf{R}_n(t) + \mathbf{f}_n\delta_{nN} \quad (n, \dots, N) \quad (43)$$

which describes the Brownian motion of a set of bonded particles whereby the last of them is subjected to external (constant) stretching force $\mathbf{f} = [f, 0, 0]$. The influence of solvent is split into slowly evolving viscous force and rapidly fluctuating stochastic force. The random, Gaussian force \mathbf{R}_n is related to friction coefficient γ by the fluctuation–dissipation theorem. The integration step is 0.002 time units (t.u.) and time is measured in units of $(m\sigma^2/\varepsilon)^{1/2}$, where m denotes the mass of the beads, $m = 1$. The ratio of the inertial forces over the friction forces in eq 43 is characterized by the Reynolds number $Re = (m\varepsilon)^{1/2}/\gamma\sigma$ which in our simulation falls in the range $Re = 0.1$ – 4 . In the course of simulation, the velocity–Verlet algorithm is used to integrate equations of motion as in eq 43.

4. SIMULATION RESULTS

In order to check the validity of our theoretical predictions, we carried out extensive computer simulations by means of both Monte Carlo (MC) and Molecular Dynamics (MD) so that a comparison can be made between the overdamped dynamics of a polymer (MC) and the behavior of an inertial (underdamped) system (MD). For ultimate consistency of the data, we performed also MD simulations with very large friction coefficient $\gamma = 10$ whereby the obtained data was found to match that from the MC computer experiment.

First of all, it would be interesting to verify that trumpet-like structures, which have been discussed thoroughly in section 2, can be seen in our MD-simulation experiment. Figure 4 represents such a visualization where the beads density distributions are given (as a function of x -coordinate as well as the radial coordinate calculated with respect to the first monomer, i.e., $r = [(y_1 - y)^2 + (z_1 - z)^2]^{1/2}$ for the weak, $\varepsilon_s/k_B T = 1.9$ (left panel), and strong, $\varepsilon_s/k_B T = 5$ (right panel), adsorptions. Each density plot was implemented as a result of averages over many runs under the fixed fraction of desorbed

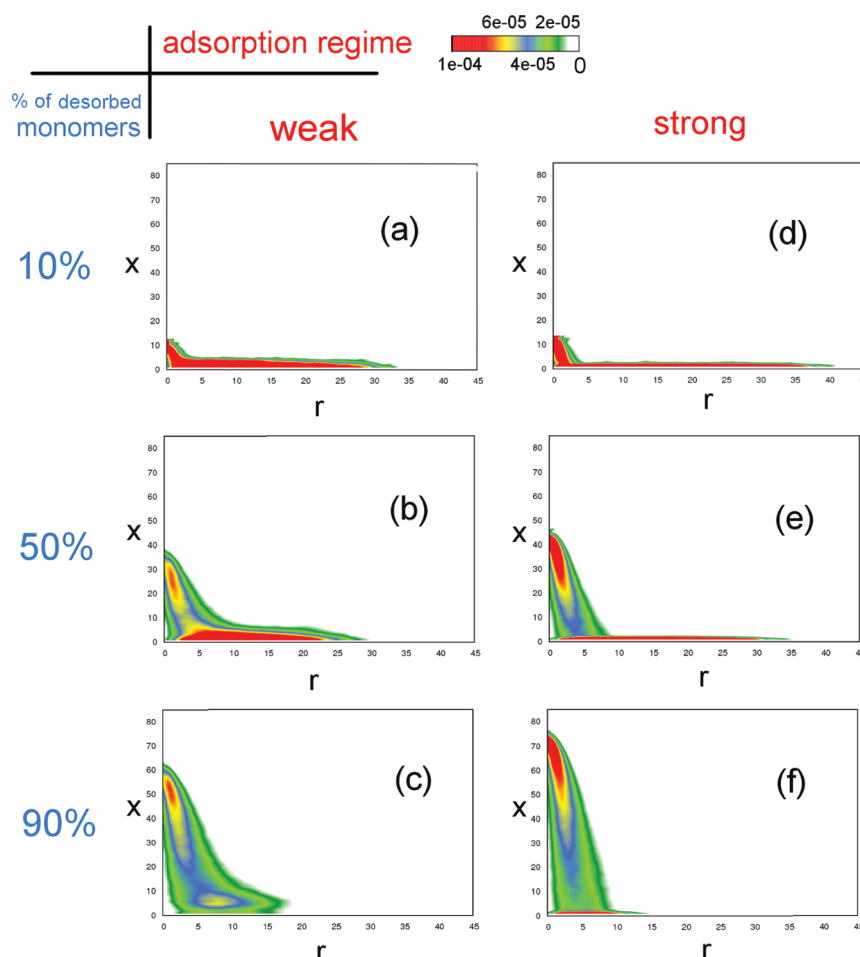


Figure 4. Polymer density distributions of beads plotted for different adsorption regimes: (a–c) $\epsilon_s/(k_B T) = 1.9$, (d–f) $\epsilon_s/(k_B T) = 5.0$ and various percentage of detached monomers (10%, 50% and 90%). The x -axis coincides with direction of pulling force whereas $r = ((y_1 - y_n)^2 + (z_1 - z_n)^2)^{1/2}$, ($n = 1, \dots, N$) is the radial component of beads calculated with respect to the first monomer. Here $N = 100$, $T = 0.1$, and $\gamma = 0.25$.

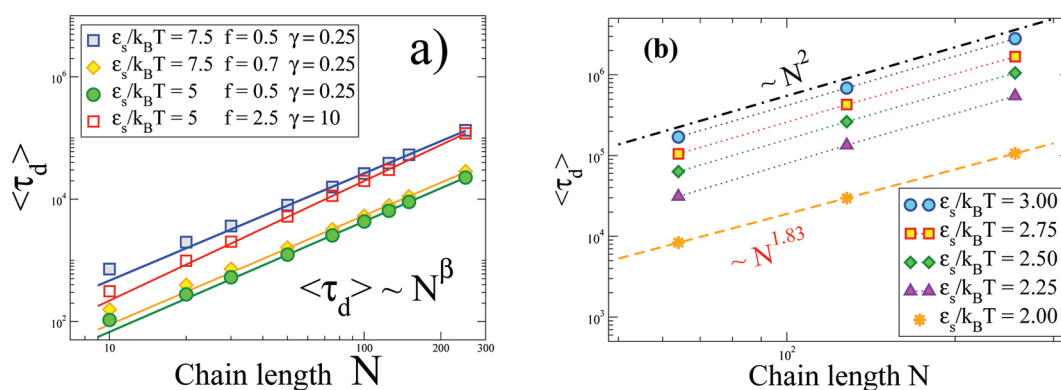


Figure 5. (a) MD data for the mean desorption time $\langle \tau_d \rangle$ of a chain vs chain length N , plotted for different strength of pulling force f , adhesion strength $\epsilon_s/k_B T$, and friction γ . Symbols denote the results of simulation while solid lines represent fitting curves $\langle \tau_d \rangle \propto N^\beta$ which were found in the range $N = 50 \div 250$. The value of the exponent β depends on the dynamics: underdamped $\beta \approx 1.75 \pm 0.1$ (full symbols) and overdamped 1.96 ± 0.03 (empty symbols). (b) Variation of $\langle \tau_d \rangle$ with N at different strength of adhesion $\epsilon_s/k_B T$ from the MC data. Note that here the critical adsorption energy $\epsilon_c/k_B T \approx 2.0$. In the strong adsorption regime $\beta = 2.0$, whereas close to the critical point $\beta = 1.83$.

monomers: 10% (upper row), 50% (middle row) and 90% (bottom row). As one can see, the moving domain is developed into the trumpet-like configuration in both, weak and strong adsorption, cases. Moreover, the “trumpet” is tilted as it was argued in section 2.1.1 due to its lateral velocity and the corresponding Stokes friction. An important point is that the tilt angle stays constant which substantially simplifies the

theoretical consideration in section 2.1.1. Recall that the density in the blob $n_b(x)$ and the blob size $\xi(x)$ are related as $n_b(x) \propto 1/[\xi(x)]^{3-1/\nu} \propto 1/[\xi(x)]^{1.3}$, i.e., the larger the density is, the smaller blob size. This tendency can be seen in Figure 4 where the most dense portion (red color) comes close to the tip of the “trumpet” as it should be. Moreover, for the strong adsorption case (see Figure 4d–f) this most dense portion

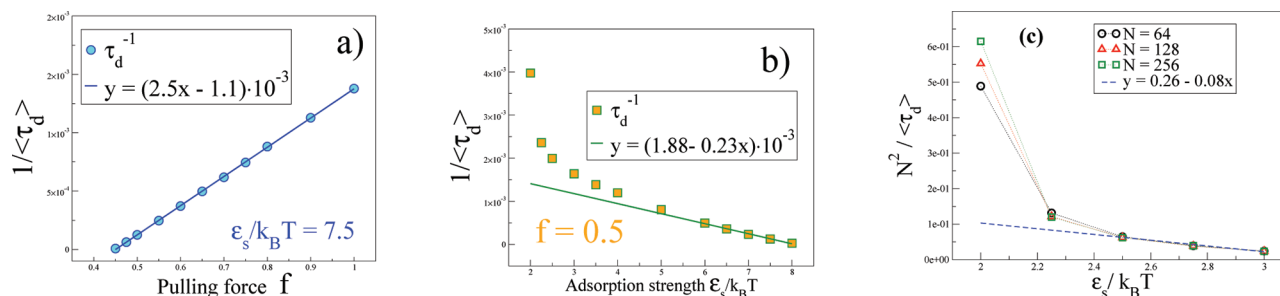


Figure 6. MD data on the inverse mean desorption time $1/\langle\tau_d\rangle$ of a chain with $N = 50$ plotted as a function of (a) pulling force f , and (b) adsorption strength $\varepsilon_s/k_B T$. Here $\gamma = 0.25$. c) Inverse mean detachment time $N^2/\langle\tau_d\rangle$ (scaled with N^2) against ε_s from MC data with $f = 3.0$ and $\varepsilon_s/k_B T = 3.0$.

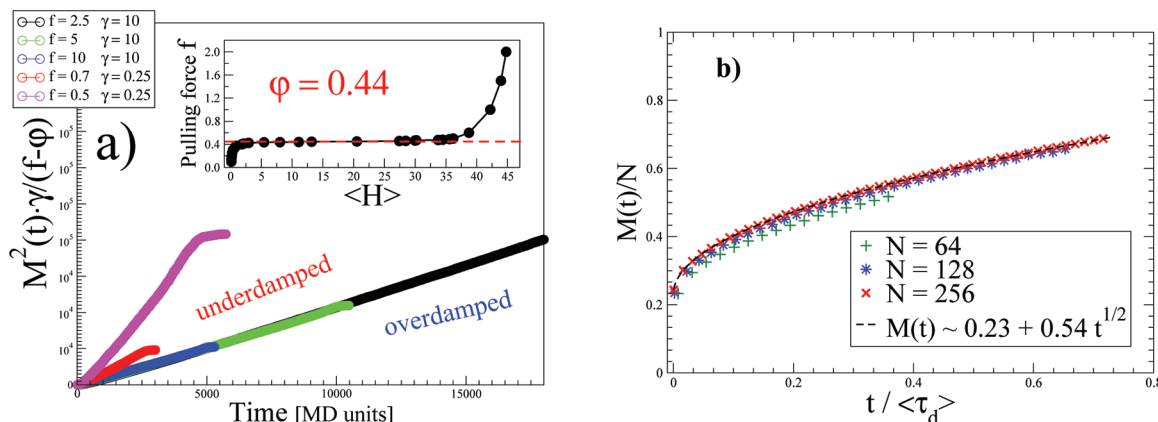


Figure 7. (a) Mean squared number of desorbed monomers $\gamma M^2(t)/[(f - \varphi)]$ for a chain composed of $N = 100$ particles shown as a function of time for different sets of f and γ -MD data. Here $\varepsilon_s/k_B T = 5.0$. The inset displays the (equilibrium) relationship between pulling force f and the resulting mean height $\langle H \rangle$ of the first monomer in a chain with $N = 50$. The estimated value of the plateau height (which is the restoring force in the course of detachment) is $\varphi = 0.44$. (b) Variation of $M(t)$ with (dimensionless) elapsed time (measured in units of $t/\langle\tau_d\rangle$) for different polymer lengths N from MC data. Here $\varepsilon_s/k_B T = 3.0$. Dashed line denotes the expected \sqrt{t} -behavior, cf. eq 33.

becomes more extended which might mean a “stem–trumpet” formation. As a result, the density plots, given in Figure 4, provide a good evidence for the existence of the trumpet-like structures, suggested and discussed in section 2.

As one of our principal results, it was found that the chain length dependence of the mean detachment time $\langle\tau_d\rangle$ follows a scaling law $\langle\tau_d\rangle \sim N^\beta$, Figure 5, where β , the detachment exponent, depends on the type of dynamics (underdamped or overdamped) as well as on the adsorption strength (i.e., on the proximity of ε_s to the adsorption critical point, ε_c). Figure 5a shows result from the MD-simulation for different values of ε_s , the pulling force f , and the friction coefficient γ . For the underdamped dynamics, one finds a detachment exponent $\beta = 1.75 \pm 0.1$ whereas for the overdamped one $\beta = 1.96 \pm 0.03$. The last value is very close to the theoretical prediction which immediately follows from eq 33, $\langle\tau_d\rangle \propto \tau_0 N^2/(\tilde{f} - \tilde{\varphi})$, i.e., $\beta = 2$. Recall that this theoretical prediction neglects any effects of inertia and describes overdamped dynamics. In addition, detachments are considered in the “stem” scenario, that is, for relatively large adsorption energy and pulling force.

This conclusion is supported by the MC-simulation results (which represent the overdamped limit) shown in Figure 5b. For the relatively strong adsorption one finds $\beta = 2.02 \pm 0.01$, which is very close to the theoretical prediction. On the other hand, in the vicinity of the adsorption critical point the detachment exponent appears to be smaller $\beta = 1.83 \pm 0.01$. Indeed, one may suggest that the observed decrease is due to fluctuations which become stronger close to ε_c . As mentioned above, fluctuations are not taken into account in our theoretical

treatment which is based on the “quasistatic” approximation. As a matter of fact, in the cases of “trumpet” and “stem–trumpet” scenarios (relatively weak adsorption energy and pulling force), the fluctuations alter the value of the detachment exponent so that $\beta < 2$. It is, however, conceivable too that $\beta = 1.83$ may also be due to finite-size effects in the vicinity of the critical adsorption point where the size of adsorption blobs becomes large.

In order to check the f - and ε_s -dependence of $\langle\tau_d\rangle$, which the relation $\langle\tau_d\rangle \propto \tau_0 N^2/(\tilde{f} - \tilde{\varphi})$ predicts for the “stem” regime, we have plotted $1/\langle\tau_d\rangle$ vs. f , Figure 6a, and vs. ε_s , Figure 6b. In Figure 6a one can see a perfect straight line as expected. As for the ε_s -dependence, we recall that according to eq 30, in the strong adsorption limit the restoring force $\tilde{\varphi} \approx c_1(\varepsilon_s + c_2)$ where c_1 and c_2 are some constants. As can be seen from Figure 6b, in the MD-simulation this holds for $\varepsilon_s > 5$. On the other hand, in the MC simulation, the strong adsorption regime starts at $\varepsilon_s > 2.5$ as is evident from Figure 6c.

Figure 7 demonstrates the validity of the \sqrt{t} -law for the time evolution of the mean number of desorbed monomers, $M(t)$, given by eq 33. According to this relationship, the quantity $\gamma M^2(t)/(f - \varphi)$ should be a linear function of time.

In order to fix the value of the restoring force φ , we have carried out an independent simulation to find how the mean height of the first monomer $\langle H \rangle$ depends in equilibrium on the pulling force f for a previously adsorbed (end-grafted) chain. The result of this is shown as an inset in Figure 7a where the value of plateau height yields the restoring force $\varphi = 0.44$ at adsorption energy $\varepsilon_s = 5.0$. By making use of this value we were

able to superimpose three curves for different forces, $f = 2.5, 5, 10$ in the overdamped case ($\gamma = 10.0$) on a single master curve as shown in Figure 7a. Evidently, in the case of underdamped dynamics this collapse on a single master curve does not work. This deviation from the theoretical predictions indicates again that they apply perfectly only to the case of overdamped dynamics. Finally, the respective $M(t)$ vs time relationship from the MC-simulation is shown in Figure 7b. One should thereby note that in the starting equilibrium configuration of the adsorbed chain about 24% of the monomers reside in loops so they are actually desorbed even before the pulling force is applied. Evidently, as in the MD data for very large friction, the curves for different chain lengths collapse on a single master \sqrt{t} -curve in agreement with eq 33.

5. CONCLUSION

In this work we consider the force-induced desorption of a polymer from a structureless adhesive surface both analytically and by means of two distinct methods for computer simulation.

We have shown theoretically that there are three dynamical regimes of a polymer chain detachment. Depending on the pulling \tilde{f} and restoring $\tilde{\varphi}$ forces, one can discriminate between a “trumpet” ($1/N^v \ll \tilde{\varphi} < \tilde{f} < 1$), “stem–trumpet” ($\tilde{\varphi} < 1 < \tilde{f}$), and “stem” ($1 < \tilde{\varphi} < \tilde{f}$) regimes of desorption.

Remarkably, in all these cases the time dependence of the number of desorbed monomers $M(t)$ and the height of the first monomer (i.e., the monomer which experiences the applied external pulling force) $R(t)$ follows an universal \sqrt{t} -law (even though this is *not* a diffusion phenomenon). There is, however, a common physical background with the well-known Lucas–Washburn \sqrt{t} -law of capillary filling²⁸ as with the ejection kinetics of a polymer chain from a cavity (virus capsid).²⁹ In these seemingly different phenomena there is always a *constant* driving force (meniscus curvature, or polymer entropy) which acts against a gradually changing drag force (friction) in the course of the process.

We discovered an interesting similarity between the differential equation governing the monomer density variation $\rho(x,t)$ in time and space, and the nonlinear porous medium equation (PME).^{17,18} This makes it possible to use the self-similarity property of PME and derive rigorously the \sqrt{t} -law. This analogy with PME and the \sqrt{t} -law behavior have been discussed recently in the context of a polymer chain gragging in a viscous fluid.³⁰

Our extensive MD- and MC-simulations of the detachment kinetics support this finding as well as the $\langle \tau_d \rangle \propto N^\beta$ scaling with $\beta = 2$ of mean detachment time τ_d with chain length N . The theoretically predicted dependence of $\langle \tau_d \rangle$ on pulling force f and adsorption energy ε_s appears in perfect agreement with the simulation results. As noted above, the consistency between theory and computer experiment is well manifested in the case of overdamped dynamics and strong adsorption. Moreover, by means of MD-simulation we have shown that the beads density distribution plots support the notion of trumpet-like tilted tensile blob structures. One can envisage not only tilted but, e.g., bended (horn-like) structures where the local lateral velocity depends on the x -coordinate. We leave this more complicated case for future investigation.

The deviations in the exponent β due to inertial effects in the underdamped dynamical regime ($\beta \approx 1.75$ found in the MD simulation) as well as close to the adsorption critical point ε_c ($\beta = 1.83$, in the MC simulation) are also challenging. It appears possible that inertial effects and fluctuations close to the CAP

(both neglected in our theoretical treatment) may lead to similar consequences for the dynamics of polymer desorption, manifested by the observed decrease in the detachment exponent β . In both cases this suggests that polymer detachment is facilitated. This is clearly a motivation for further studies of the problem.

AUTHOR INFORMATION

Corresponding Author

*E-mail: jaturej@univ.szczecin.pl

Notes

The authors declare no competing financial interest.

ACKNOWLEDGMENTS

We thank K. L. Sebastian, H.-J. Butt, K. Koyanov, and M. Baumgarten for helpful discussions. A.M. is indebted to the Max-Planck Institute for Polymer Research in Mainz, Germany, for hospitality during his visit and to CECAM-Mainz for financial support. This work has been supported by the Deutsche Forschungsgemeinschaft (DFG), Grant No. SFB 625/B4.

REFERENCES

- Ritort, F. *J. Phys. Condens. Matter* **2006**, *18*, R531.
- Bhattacharjee, S. M. *J. Phys. A* **2000**, *33*, L423.
- Marenduzzo, D.; Trovato, A.; Maritan, A. *Phys. Rev. E* **2001**, *64*, 031901.
- Orlandini, E.; Bhattacharjee, S.; Marenduzzo, D.; Maritan, A.; Seno, F. *J. Phys. A* **2001**, *34*, L751.
- Kierfeld, J. *Phys. Rev. Lett.* **2006**, *97*, 058302.
- Sebastian, K. L. *Phys. Rev. E* **2000**, *62*, 1128.
- Marenduzzo, D.; Bhattacharjee, S. M.; Maritan, A.; Orlandini, E.; Seno, F. *Phys. Rev. Lett.* **2002**, *88*, 028102.
- Bhattacharya, S.; Rostiasvili, V. G.; Milchev, A.; Vilgis, T. *Phys. Rev. E* **2009**, *79*, 030802(R).
- Bhattacharya, S.; Rostiasvili, V. G.; Milchev, A.; Vilgis, T. *Macromolecules* **2009**, *42*, 2236.
- Bhattacharya, S.; Milchev, A.; Rostiasvili, V. G.; Vilgis, T. *Eur. Phys. J. E* **2009**, *29*, 285.
- Skvortsov, A. M.; Klushin, L. I.; Fleer, G. J.; Leermakers, F. A. M. *J. Chem. Phys.* **2010**, *132*, 064110.
- Brochard-Wyart, F. *Europhys. Lett.* **1993**, *23*, 105.
- Sakaue, T. *Phys. Rev. E* **2007**, *76*, 021803.
- Sakaue, T. *Phys. Rev. E* **2010**, *81*, 041808.
- Sebastian, K. L.; Rostiasvili, V. G.; Vilgis, T. A. *EPL* **2011**, *95*, 48006.
- Simsen, J.; Gentile, C. B. *Nonlinear Anal.* **2009**, *71*, 4609.
- Vázquez, J. L. *The Porous Medium Equation*; Clarendon Press: Oxford, U.K., 2007.
- Barenblatt, G. I.; Entov, V. M.; Ryzhik, V. M. *Theory of Fluid Flows Through Natural Rocks*; Kluwer Academic Publishers: London, 1990.
- de Gennes, P. G.; Pincus, P. *J. Phys. (Fr.) Lett.* **1983**, *44*, L241.
- de Gennes, P. G. *Scaling Concept in Polymer Physics*; Cornell University Press: Ithaca, NY, 1979.
- Sakaue, T.; Yoshinaga, N. *Phys. Rev. Lett.* **2009**, *102*, 148302.
- Serr, A.; Netz, R. *Europhys. Lett.* **2006**, *73*, 292.
- Bhattacharya, S.; Milchev, A.; Rostiasvili, V. G.; Vilgis, T. A. *Eur. Phys. J. E* **2009**, *29*, 285.
- Bhattacharya, S.; Milchev, A.; Rostiasvili, V. G.; Vilgis, T. A. *Macromolecules* **2009**, *42*, 2236.
- Vanderzande, C. *Lattice Model of Polymers*; Cambridge University Press: Cambridge, U.K., 1998.
- Sheng, Y.-J.; Lai, P.-Y. *Phys. Rev. E* **1997**, *56*, 1900.
- Milchev, A.; Binder, K. *Macromolecules* **1996**, *29*, 343.

- (28) Dimitrov, D. I.; Klushin, L.; Milchev, A.; Binder, K. *Phys. Fluids* **2008**, *20*, 092102.
- (29) Milchev, A.; Klushin, L.; Skvortsov, A.; Binder, K. *Macromolecules* **2010**, *43*, 6877.
- (30) Sakaue, T.; Saito, T.; Wada, H. arXiv:1203.4095v1.